scientific reports

OPEN

Predicting the total PAHs concentrations in sediments from selected congeners using a multiple linear relationship

Weiwei Wang[1,2,3], Huaping Xu[4], Xiaolei Qu[5], Kun Yang[1,2,3,6✉] & Daohui Lin[1,2,3]

In this study, we observed that four congeners, including naphthalene (Nap), acenaphthylene (Acy), phenanthrene (Phe), and benz(a)anthracene (BaA), are the characteristic congeners for predicting the emission and the sediment concentrations of polycyclic aromatic hydrocarbons (PAHs). A novel multiple relationship of the total PAHs concentrations ($C_{\Sigma PAHs}$) in sediments with the concentrations of four congeners was established ($p < 0.01$, $R^2 = 0.95$) using published data over the past 30 years. Moreover, the multiple linear relationship of the total PAHs emission factors with the emission factors of four congeners was also established ($p < 0.01$, $R^2 = 0.99$). Interestingly, the ratio of multicomponents coefficient from the multiple linear relationship in sediments to that from the multiple linear relationship in emission sources correlated positively with octanol–water partition coefficient ($\log K_{ow}$) ($p < 0.01$, $R^2 = 0.88$) of the four PAHs congeners. Therefore, a novel model was established to predict $C_{\Sigma PAHs}$ in sediments using the emissions and $\log K_{ow}$ of the four characteristic PAHs congeners. The percent sample deviation between calculated $C_{\Sigma PAHs}$ and their observed values was 54%, suggesting the established model can accurately predict $C_{\Sigma PAHs}$ in sediments.

Polycyclic aromatic hydrocarbons (PAHs) are a group of persistent organic contaminants that originate from the incomplete combustion of organic matter (such as biomass and coal) and non-combustion emissions of petrogenic processes[1–3]. United States Environmental Protection Agency (USEPA) and European Union (EU) have identified sixteen PAHs (Table S1) as priority pollutants due to their toxicity and risks to human health and the environment[4–7]. For example, PAHs in sediments can pose detrimental effects on benthic organisms and pelagic organisms[8,9]. Therefore, PAHs concentrations in sediments have been widely investigated in the past decades for assessing their risks[10–18]. The common method for the quantification of PAHs in sediments is chromatography, including gas chromatography or liquid chromatography, coupled with mass spectrometry[19–21]. However, the whole process of chromatographic analysis for PAHs in sediments is tedious and cost-consuming. Moreover, this method may be potentially damaging for the environment because the analysis typically requires a pre-concentration procedure, which may use large volumes of organic solvents for extraction and clean-up[22–24]. For example, the frequently used organic solvents, dichloromethane[19–21], can damage human nervous system and even the functions of liver and kidney through skin mucosa and nasal breathing[25,26]. Therefore, it is necessary to establish correlations that can be applied to predict concentrations of PAHs in sediments for cutting costs and saving time in laboratory analysis[27,28].

In recent literatures, significantly positive correlations between the total concentration of PAHs ($C_{\Sigma PAHs}$) and the content of total organic carbon (f_{oc}) in sediments were established to predict $C_{\Sigma PAHs}$[17,29–31], built on the premise that the distribution of PAHs between sediments and water is largely depended on the partitioning of PAHs into sediment organic matter[32]. However, our preliminary work indicated that $C_{\Sigma PAHs}$ predicted using f_{oc} (Eq. 1) does not hold true for additional $C_{\Sigma PAHs}$ and f_{oc} data of 233 global sediment samples (Fig. 1a, Table S2), presented by the low determination coefficients ($R^2 = 0.20$) and the great percent sample deviation (SDEV = 771%). One

[1]Department of Environmental Science, Zhejiang University, Hangzhou 310058, China. [2]Key Laboratory of Environmental Pollution and Ecological Health of Ministry of Education, Hangzhou 310058, China. [3]Zhejiang Provincial Key Laboratory of Organic Pollution Process and Control, Hangzhou 310058, China. [4]Mathematics Teaching and Research Section, College of Pharmaceutical Sciences, Zhejiang Chinese Medical University, Hangzhou 310053, China. [5]State Key Laboratory of Pollution Control and Resource Reuse, School of the Environment, Nanjing University, Jiangsu 210023, China. [6]Zhejiang University-Hangzhou Global Scientific and Technological Innovation Center, Hangzhou 311200, China. ✉email: kyang@zju.edu.cn
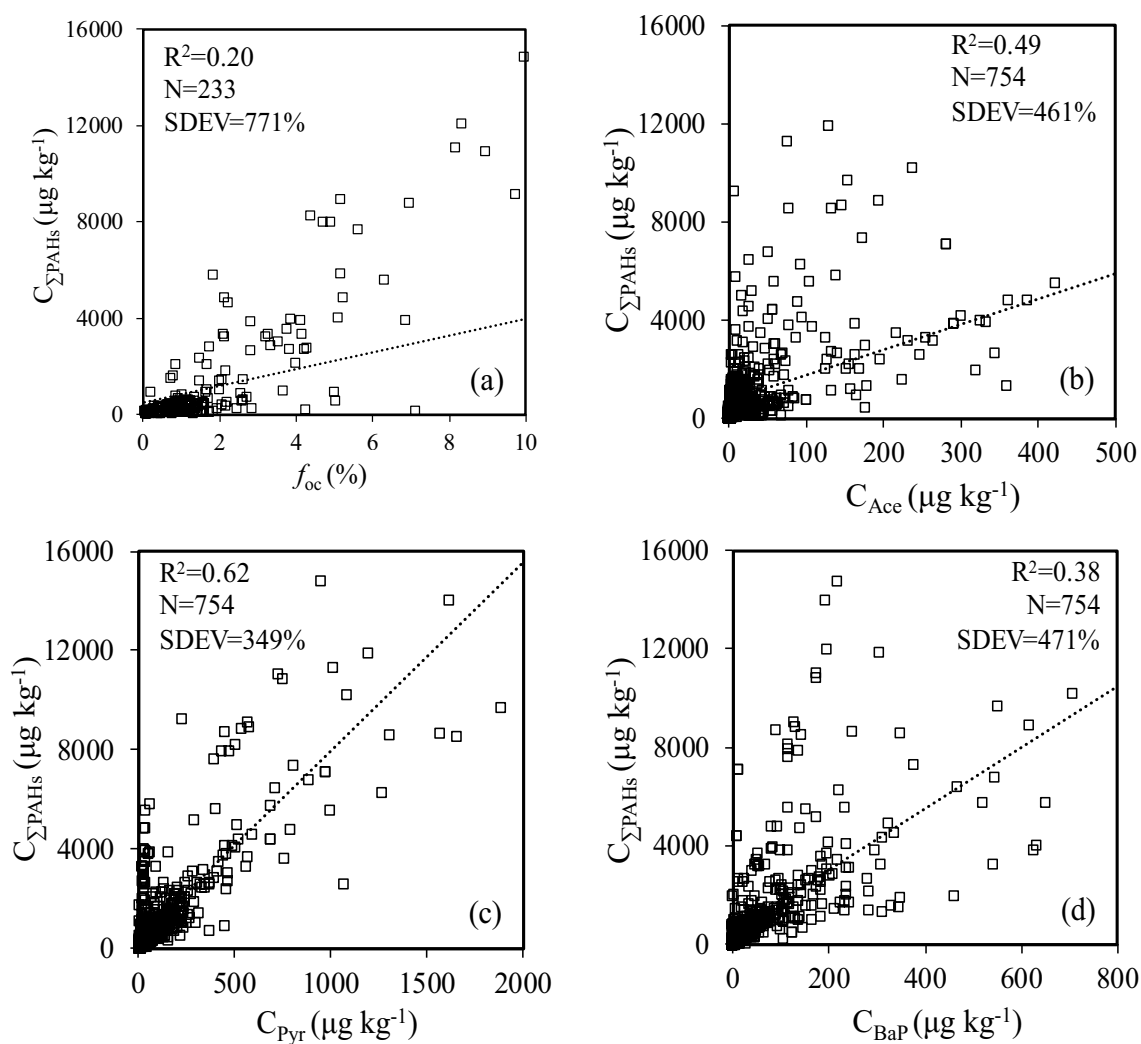
Figure 1. Linear relationships of $C_{\Sigma PAHs}$ with f_{oc} (**a**), $C_{(Ace)}$ (**b**), $C_{(Pyr)}$ (**c**) or $C_{(BaP)}$ (**d**). Dashed lines in the plots are linear regressions.

possible reason for the insignificant correlation between $C_{\Sigma PAHs}$ and f_{oc} when more data was introduced is that the difference in emissions of PAHs in various regions is ignored. Another possible reason is that the dependence of PAHs partitioning in sediment organic matter and their polarity is ignored[4,32,33]. Furthermore, nonlinear sorption of PAHs on sediments organic matter is also ignored[34,35].

Intrinsic quantitative relationships between $C_{\Sigma PAHs}$ and the concentrations of single PAHs congener were also established to predict sediment $C_{\Sigma PAHs}$ in previous studies[36–39]. For example, the concentration of benzo(a) pyrene (C_{BaP})[36,37], pyrene (C_{Pyr})[38] or acenaphthene (C_{Ace})[39] was suggested to predict $C_{\Sigma PAHs}$ (Table S3). However, when relationships of $C_{\Sigma PAHs}$ with C_{BaP} (Eq. 2), C_{Pyr} (Eq. 3) and C_{Ace} (Eq. 4) were established using the additional sediment concentration data of PAHs from China (Table S4), it was found that the relationships were less significant with greater deviation (Eqs. 2–4). For example, R^2 of the linear relationship between $C_{\Sigma PAHs}$ and C_{Ace} (Eq. 4) reduced from 0.82[39] to 0.49 (Eq. 4) with SDEV increased from 27%[39] (Table S3) to 461% (Eq. 4), when sediment sample numbers (N) increased from 10[39] (Table S3) to 754 (Eq. 4), respectively. A possible reason for these relationships (Eqs. 2–4) predicted with less accuracy is that the difference in emission factors (EFs) of PAHs congeners for various sources is ignored. For example, at the equivalent emission factors of the total PAHs ($EF_{\Sigma PAHs}$), which is 4.39 g t^{-1} for iron sintering and 4.51 g t^{-1} for gasoline combustion (Table 1), EF of Ace (Table 1) from iron sintering is 0.079 g t^{-1}, about 2 orders of magnitude larger than that 0.00046 g t^{-1} of gasoline combustion[40,41]. Therefore, the concentrations of single PAHs congener cannot be used to accurately predict $C_{\Sigma PAHs}$ in sediments on a large scale. The characteristic PAHs congeners in emission sources and in sediments should be explored to develop an accurate model for predicting $C_{\Sigma PAHs}$ in sediments.

$$C_{\Sigma PAHs} = 351.75(\pm 39.67) \times f_{oc} + 455.13(\pm 132.48)$$
$$\left(R^2 = 0.20, p = 0.13, N = 233, SDEV = 771\% \right)$$

(1)

EFs	PAHs	R^2	p value
Σ 1st subgroup	Nap	1.00	<0.01
Σ 2nd subgroup	Acy	1.00	<0.01
Σ 3rd subgroup	Ace	0.87	<0.01
	Flo	0.97	<0.01
	Phe	0.98	<0.01
	Ant	0.96	<0.01
	Flu	0.97	<0.01
	Pyr	0.91	<0.01
Σ 4th subgroup	BaA	0.98	<0.01
	Chr	0.97	<0.01
	BbF	0.94	<0.01
	BkF	0.92	<0.01
	BaP	0.94	<0.01
	IcdP	0.88	<0.01
	BghiP	0.87	<0.01
	DahA	0.77	<0.01

Table 1. Coefficient of determination (R^2) and significance (p) of emission factors (EFs) of individual PAHs congeners with the total EFs of PAHs congeners in four subgroups for various emission sources.

$$C_{\Sigma PAHs} = 12.50(\pm0.59) \times C_{BaP} + 512.96(\pm76.53)$$
$$\left(R^2 = 0.38, p < 0.01, N = 754, SDEV = 471\%\right) \tag{2}$$

$$C_{\Sigma PAHs} = 7.16(\pm0.15) \times C_{pyr} + 340.26(\pm45.20)$$
$$\left(R^2 = 0.62, p < 0.01, N = 754, SDEV = 349\%\right) \tag{3}$$

$$C_{\Sigma PAHs} = 10.48(\pm0.41) \times C_{Ace} + 765.57(\pm71.31)$$
$$\left(R^2 = 0.49, p < 0.01, N = 754, SDEV = 464\%\right) \tag{4}$$

In this study, a multiple linear relationship between $EF_{\Sigma PAHs}$ and the EFs of characteristic congeners was established by identifying characteristic PAHs congeners in emission sources. Moreover, another multiple linear relationship between $C_{\Sigma PAHs}$ and the concentrations of characteristic congeners in sediments was established by identifying characteristic PAHs congeners in sediments. Finally, an accurate model for predicting $C_{\Sigma PAHs}$ in sediments was established by exploring the correlation between the sediment concentrations and the emissions of characteristic PAHs congeners. The established model can cut costs and save time in PAHs analysis for risk assessing of PAHs in the sediment environment.

Result and discussion

Characteristic congeners of PAHs in emission. Hierarchical clustering analysis (HCA) and classifications for relative similarities[42,43] of PAHs emission factors (Table S5) show that sixteen PAHs can be divided into four groups (Table 1, Fig. 2). The first subgroup is Nap (Table 1, Fig. 2) because of its highest EFs in most emission sources (Table S5). Acy is the second subgroup (Table 1, Fig. 2) with significant lower EFs than that of Nap but higher than other PAHs congeners in most emission sources (Table S5). The third subgroup comprises four 3-ring PAHs (Ace, Flo, Phe and Ant) and two 4-ring PAHs (Pyr and Flu) (Fig. 2, Table 1). In this subgroup, the EFs of Phe (EF_{Phe}) has the best linear correlation with the total EFs of this subgroup, showing the maximum R^2 of 0.98 (N = 15, $p < 0.01$) (Table 1). Thus, the total EFs of the third subgroup can be expressed by EF_{Phe} with the largest degree of accuracy[43,44]. The last subgroup is composed of the other eight PAHs congeners (Fig. 2, Table 1), including 4-ring PAHs (BaA and Chr) and 5, 6-ring PAHs (BbF, BkF, BaP, IcdP, DahA and BghiP). The EFs of BaA (EF_{BaA}) correlates best with the total EFs of the eight PAHs in this subgroup with the maximum R^2 of 0.98 (N = 15, $p < 0.01$) (Table 1). This indicates that the total EFs of the last subgroup can be presented by EF_{BaA}. Moreover, the total EFs of sixteen PAHs ($EF_{\Sigma PAHs}$) are well related with EF_{Nap}, EF_{Acy}, EF_{Phe}, and EF_{BaA} in a multilinear relationship (Eq. 5 and Fig. 3), having R^2 of 0.99, high F values of 5257, and low SDEV of 24%. Therefore, Nap, Acy, Phe, and BaA can be employed as characteristic congeners of sixteen PAHs in emission sources (Fig. 3).

$$EF_{\sum PAHs} = -0.45(\pm0.46) + 0.98(\pm0.12) \times EF_{Nap} + 1.12(\pm0.11) \times EF_{Acy}$$
$$+ 2.82(\pm0.23) \times EF_{Phe} + 4.04(\pm0.47) \times EF_{BaA}$$
$$\left(N = 15, R^2 = 0.99, F = 5257, SDEV = 24\%\right) \tag{5}$$
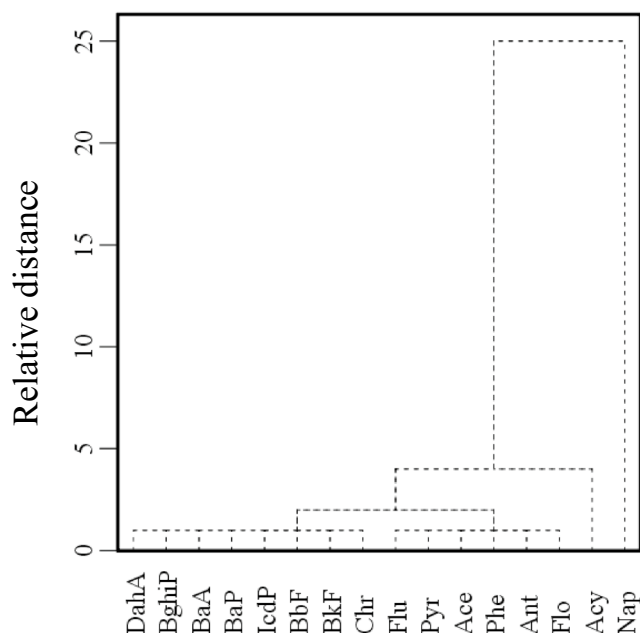
Figure 2. Hierarchical clustering analysis dendrograms of emission factors of sixteen PAHs in emission sources using average linkage clustering between clusters.
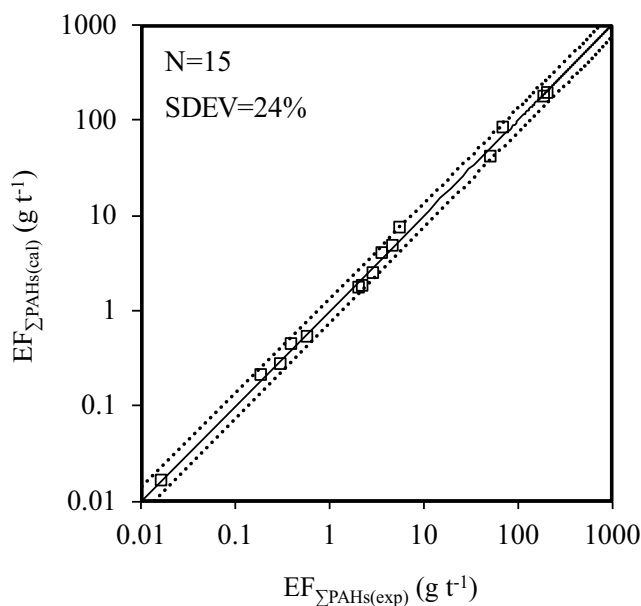

Figure 3. Fitted $EF_{\Sigma PAHs(cal)}$ versus $EF_{\Sigma PAHs(exp)}$ from nine PAHs emission sources. The y = x line (solid line) indicates a 1:1 relationship between $EF_{\Sigma PAHs(cal)}$ and $EF_{\Sigma PAHs(exp)}$. Dashed lines in the plot indicate the SDEV values from the reference line.

Characteristic congeners of PAHs in sediments. The HCA dendrogram for correlations of sixteen PAHs in sediments of China is shown in Fig. 4. When PAHs are classified into two groups, the first subgroup is composed of 2, 3-rings PAHs and two 4-rings PAHs (Table 2). In this subgroup, the concentration of Phe (C_{Phe}) correlates best with the total concentration of the eight congeners with the maximum R^2 of 0.83 (N = 754, $p < 0.01$) (Table 2). The other two 4-rings PAHs and 5, 6-rings PAHs are divided into the second subgroup (Table 2). In the second subgroup, the maximum value of R^2 was found between the concentration of BaA (C_{BaA}) and the total concentration of the eight congeners ($R^2 = 0.79$, N = 754, $p < 0.01$) (Table 2). Thus, the total concentration of PAHs in two subgroups can be expressed by C_{Phe} and C_{BaA} with the largest degree of accuracy,
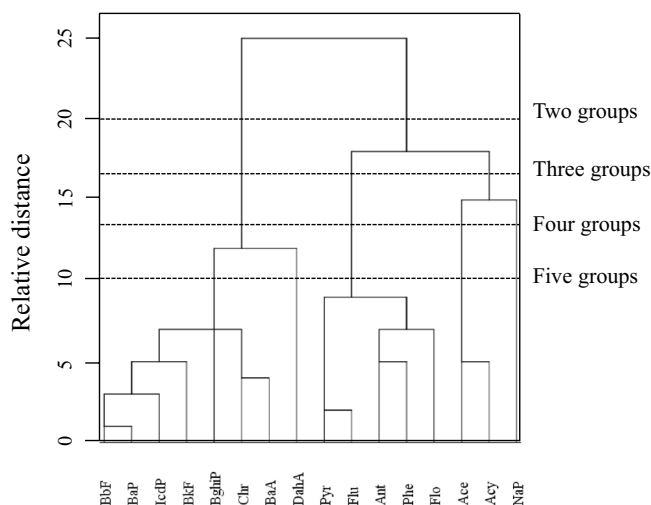
Figure 4. Hierarchical clustering analysis dendrograms of sixteen PAHs concentrations in sediments using average linkage clustering between clusters.

Two groups	PAHs	R^2	Three groups	PAHs	R^2	Four groups	PAHs	R^2	Five groups	PAHs	R^2
Σ 1st subgroup	Nap	0.45	Σ 1st subgroup	Nap	0.71	Σ 1st subgroup	Nap	1.00	Σ 1st subgroup	Nap	1.00
	Acy	0.58		Acy	0.62	Σ 2nd subgroup	Acy	0.62	Σ 2nd subgroup	Acy	0.62
	Ace	0.26		Ace	0.49		Ace	0.53		Ace	0.53
	Flo	0.73	Σ 2nd subgroup	Flo	0.69	Σ 3rd subgroup	Flo	0.69	Σ 3rd subgroup	Flo	0.69
	Phe	0.83		Phe	0.88		Phe	0.88		Phe	0.88
	Ant	0.72		Ant	0.66		Ant	0.66		Ant	0.66
	Flu	0.67		Flu	0.75		Flu	0.75		Flu	0.75
	Pyr	0.66		Pyr	0.78		Pyr	0.78		Pyr	0.78
Σ 2nd subgroup	BaA	0.79	Σ 3rd subgroup	BaA	0.79	Σ 4th subgroup	BaA	0.79	Σ 4th subgroup	BaA	0.77
	Chr	0.75		Chr	0.75		Chr	0.75		Chr	0.76
	BbF	0.66		BbF	0.66		BbF	0.66		BbF	0.68
	BkF	0.75		BkF	0.75		BkF	0.75		BkF	0.74
	BaP	0.64		BaP	0.64		BaP	0.64		BaP	0.64
	IcdP	0.57		IcdP	0.57		IcdP	0.57		IcdP	0.58
	BghiP	0.74		BghiP	0.74		BghiP	0.74		BghiP	0.73
	DahA	0.59		DahA	0.59		DahA	0.59	Σ 5th Subgroup	DahA	1.00

Table 2. Correlation coefficient (R^2) between the concentration of single congener and total congeners in each subgroup when sixteen PAHs congeners were divided into two-five groups.

respectively[43,44]. Relationship of C_{Phe} and C_{BaA} with $C_{\Sigma PAHs}$ was established in Eq. (6). Similarly, when 16 PAHs were classified into three groups, the concentration of Nap (C_{Nap}), Phe (C_{Phe}), and BaA (C_{BaA}) correlate best with the total concentrations of congeners in corresponding subgroup (Table 2). Relationship of C_{Nap}, C_{Phe}, and C_{BaA} with $C_{\Sigma PAHs}$ was established in Eq. (7). When sixteen PAHs were classified into four groups, C_{Nap}, C_{Acy}, C_{Phe}, and C_{BaA} correlate best with the total concentrations of congeners in corresponding subgroup (Table 2). Relationship of C_{Nap}, C_{Acy}, C_{Phe}, and C_{BaA} with $C_{\Sigma PAHs}$ was established in Eq. (8). When sixteen PAHs were classified into five groups, C_{Nap}, C_{Acy}, C_{Phe}, C_{BaA}, and the concentration of DahA (C_{DahA}) correlate best with the total concentrations of congeners in corresponding subgroup (Table 2). Relationship of C_{Nap}, C_{Acy}, C_{Phe}, C_{BaA} and C_{DahA} with $C_{\Sigma PAHs}$ was established in Eq. (9). Correlations between the calculated $C_{\Sigma PAHs}$ ($C_{\Sigma PAHs(cal)}$) and the experimental value ($C_{\Sigma PAHs(exp)}$) are presented in Fig. 5. SDEV values between $C_{\Sigma PAHs(cal)}$ and $C_{\Sigma PAHs(exp)}$ in Fig. 5a–d were 124%, 75%, 35% and 37%, respectively. SDEV values decreased significantly from Fig. 5a–c, while almost remained constant from Fig. 5c, d. Intercepts in equations presented the same tendency to SDEV value (Fig. 5). $C_{\Sigma PAHs}$ can't be accurately predicted using two (Fig. 5a) or three congeners (Fig. 5b), especially when $C_{\Sigma PAHs}$ in sediments lower than the intercepts in Eqs. (6–7). Four (Fig. 5c) or five congeners (Fig. 5d) can accurately predict $C_{\Sigma PAHs}$. However, more work needs to be done to complete the prediction of five congeners than four congeners. In summary, $C_{\Sigma PAHs}$ can be well predicted from the concentration of Nap, Acy, Phe, and BaA using the linear relationship of Eq. (8) (Fig. 5c).
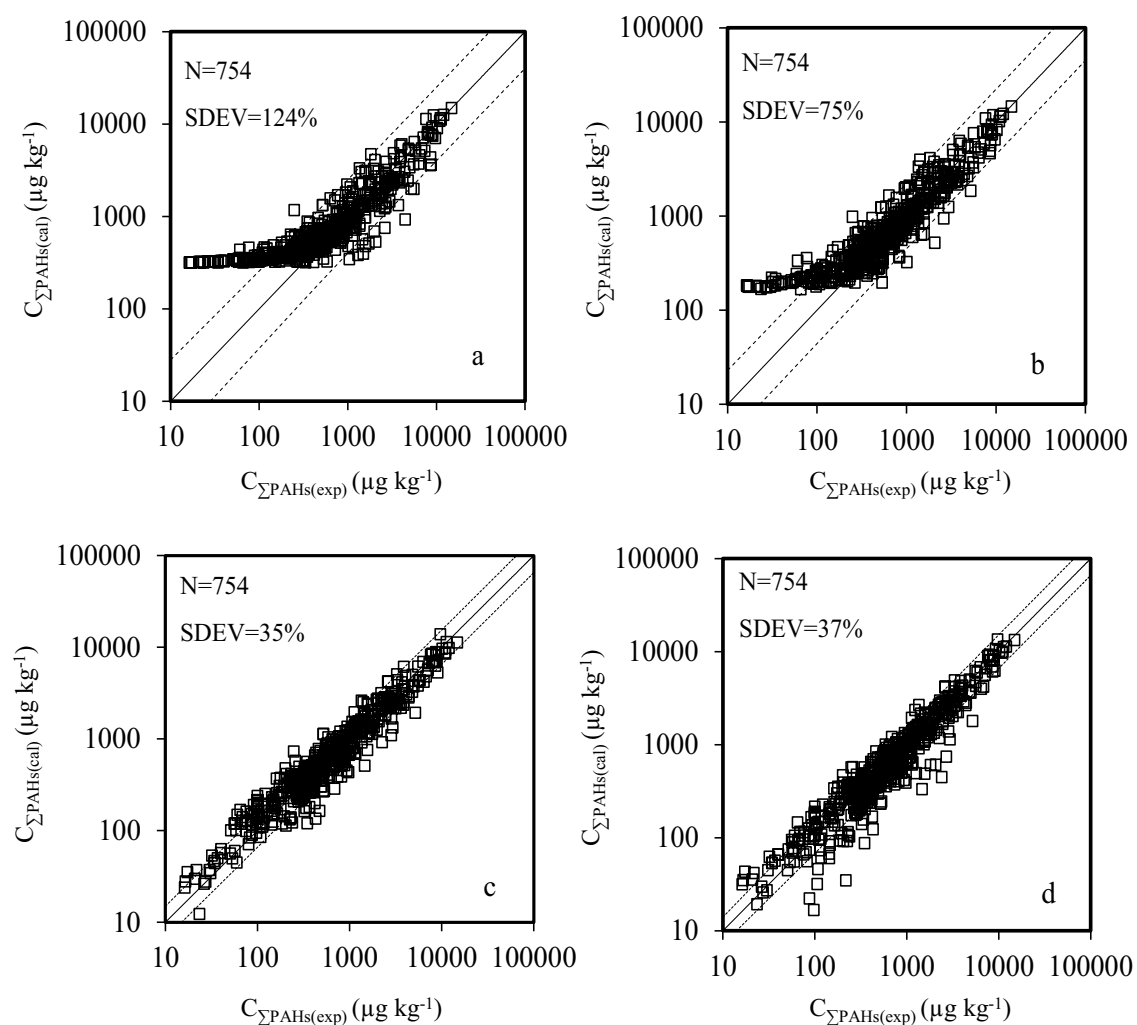
Figure 5. Fitted $C_{\Sigma PAHs(cal)}$ values from two groups (**a**), three groups (**b**), four groups (**c**) and five groups (**d**) versus $C_{\Sigma PAHs(exp)}$ values in sediments sampled in China. The y = x line (solid lines) indicates a 1:1 relationship between $C_{\Sigma PAHs(cal)}$ and $C_{\Sigma PAHs(exp)}$. Dashed lines in the plots indicate the SDEV values from the reference lines.

$$C_{\Sigma PAHs} = 245.62(\pm 28.67) + 3.92(\pm 0.10) \times C_{Phe} + 4.71(\pm 0.20) \times C_{BaA}$$
$$\left(N = 754, \ R^2 = 0.83, \ F = 2190, \ SDEV = 124\%\right) \tag{6}$$

$$C_{\Sigma PAHs} = 124.27(\pm 25.88) + 1.81(\pm 0.11) \times C_{Nap}$$
$$+ 3.43(\pm 0.14) \times C_{Phe} + 4.67(\pm 0.23) \times C_{BaA}$$
$$\left(N = 754, \ R^2 = 0.89, \ F = 2348, \ SDEV = 75\%\right) \tag{7}$$

$$C_{\Sigma PAHs} = 22.62(\pm 11.78) + 0.84(\pm 0.07) \times C_{Nap} + 1.23(\pm 0.13) \times C_{Acy}$$
$$+ 3.78(\pm 0.15) \times C_{Phe} + 5.97(\pm 0.22) \times C_{BaA}$$
$$\left(N = 754, \ R^2 = 0.95, \ F = 2740, \ SDEV = 35\%\right) \tag{8}$$

$$C_{\Sigma PAHs} = 33.34(\pm 19.89) + 0.76(\pm 0.14) \times C_{Nap} + 1.31(\pm 0.32) \times C_{Acy}$$
$$+ 3.43(\pm 0.12) \times C_{Phe} + 4.54(\pm 0.30) \times C_{BaA} + 1.50(\pm 0.51) \times C_{DahA}$$
$$\left(N = 754, \ R^2 = 0.96, \ F = 2557, \ SDEV = 37\%\right) \tag{9}$$

Prediction of total PAHs concentrations in sediments with characteristic PAHs congeners. With the established multiple linear relationship (Eq. 8), we found that the total PAHs concentrations
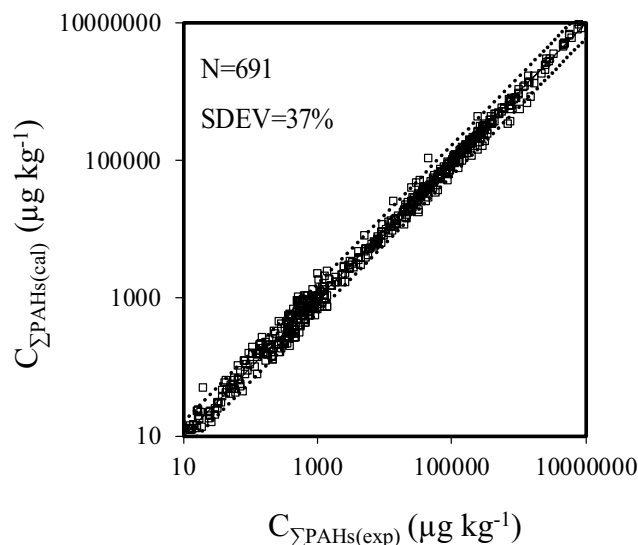
Figure 6. Fitted $C_{\Sigma PAHs(cal)}$ versus $C_{\Sigma PAHs(exp)}$ in sediments sampled in globe excluding China. The y = x line (solid line) indicates a 1:1 relationship between $C_{\Sigma PAHs(cal)}$ and $C_{\Sigma PAHs(exp)}$. Dashed lines in the plots indicate the SDEV values from the reference lines.

($C_{\Sigma PAHs}$) in sediments can be predicted from the concentrations of four characteristic congeners with high R^2 but low SDEV value. Figure 5c shows that $C_{\Sigma PAHs(cal)}$ are consistent with $C_{\Sigma PAHs(exp)}$ in sediments sampled in China. Scatterplots of unstandardized residuals (the difference between $C_{\Sigma PAHs(cal)}$ and $C_{\Sigma PAHs(exp)}$) with C_{Nap}, C_{Acy}, C_{Phe} or C_{BaA} in sediments distributed regularly on both sides of the horizontal line and no obvious positive or negative trend existed (Fig. S1). This indicates the significant stability of the established linear relationship[45]. Furthermore, $C_{\Sigma PAHs(cal)}$ also agreed well with $C_{\Sigma PAHs(exp)}$ using additional concentration data (Table S6) in sediment samples from elsewhere around the globe (N = 691) (Fig. 6), suggesting that the relationship can be applied to predict $C_{\Sigma PAHs}$ in sediments that are not only localized in China. Therefore, Nap, Acy, Phe, and BaA can be also employed as characteristic congeners of sixteen PAHs in sediments.

The same characteristic congeners observed for PAHs in sediments and in emission sources indicates that the concentration of PAHs in sediments are largely depended on their emission, which was consistent with the reported results[46–48]. In previous studies[17,29–31], PAHs emissions were not involved in the relationship of predicting PAHs concentration in sediments using f_{oc} (Eq. 1), which does not hold true in some cases. For example, for a given f_{oc}, $C_{\Sigma PAHs}$ in sediments can vary by 1–3 orders of magnitude (Fig. 1a) because of the difference in PAHs emissions in various regions. For another example, although the mean f_{oc} (6.4%) in sediments from the upper reach of Huaihe River[50] was higher than that in sediments from the lower reach of Huaihe River (f_{oc} = 4.1%)[51], $C_{\Sigma PAHs}$ in sediments from the lower reach of Huaihe River (mean value = 1721.7 µg kg^{-1})[50] were higher than that from the upper reach (mean value = 400.5 µg kg^{-1})[51]. This can be attributed to the higher emission intensity of PAHs in lower reach of Huaihe River region than that in the upper reach region[41,52,53]. Moreover, a significantly positive correlation between mean concentrations of thirteen PAHs (except for Nap, Acy, and Ace) in sediment samples derived from globe (N = 1445) and their mean EFs in fifteen emission divisions was also observed (Fig. S2), indicating that the concentration of PAHs in sediments also mainly depends on the PAHs emission. The deviation of Nap, Acy, and Ace from the linear relationship in Fig. S2 can be attributed to their relatively low $\log K_{ow}$ but high S_w (Table S1), making them not be readily adsorbed by organic matters in sediments but tend to be more readily dissolved in water[48].

Relationship between PAHs concentrations in sediments and EFs in emission sources. Significance of multicomponent coefficients in Eqs. (5) and (8) were less than 0.05 ($p < 0.05$), which are statistically significant. However, significance of intercept in Eq. (5) was greater than 0.05 ($p > 0.05$), which is statistically insignificant. The significant intercept ($p < 0.05$) in Eq. (8) can be assigned to background concentrations of PAHs in sediments[54,55]. Moreover, significantly positively linear relationships of the multicomponent coefficients in Eq. (5) and that in Eq. (8) with the $\log K_{ow}$ of four characteristic congeners were observed (Fig. 7a). Interestingly, the coefficient of characteristic congeners with larger $\log K_{ow}$, such as BaA, in Eq. (8) are higher than that in Eq. (5) (Fig. 7a). This could be attributed to the influence of sorption of PAHs in sediments and their biodegradation in the environment. For PAHs with larger $\log K_{ow}$, they tend to be more readily adsorbed in sediments organic matter by partitioning than the PAHs with smaller $\log K_{ow}$[56,57]. Meanwhile, PAHs congeners with relatively low $\log K_{ow}$ tend to be more readily degraded than those with relatively high $\log K_{ow}$[58,59], presented by the positively linear relationship of PAHs $\log K_{ow}$ with their biodegradation half-life (Fig. S3). Therefore, a positively linear relationship between the ratio of multicomponents coefficient from the multiple linear relationship in sediments (Eq. 8) to that from the multiple linear relationship in emission sources (Eq. 5) and the $\log K_{ow}$ of four PAHs congeners can be observed in Fig. 7b. This suggests that the distribution of PAHs in sediments could
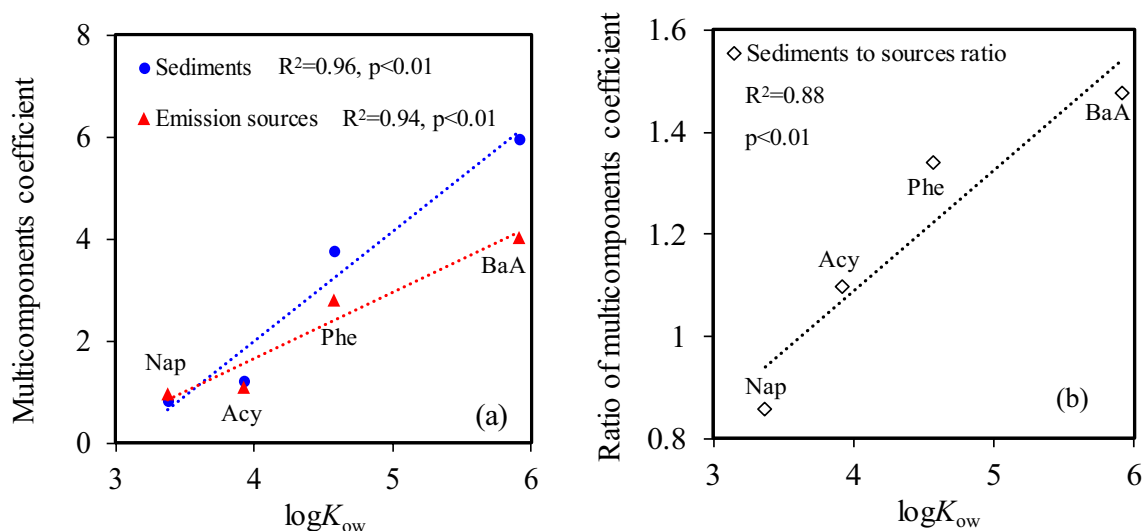
Figure 7. Relationships of multicomponents coefficients in Eq. (8) and that in Eq. (5) (**a**), as well as ratios of multicomponents coefficient in Eq. (8) to that in Eq. (5) (**b**) with the $\log K_{ow}$ of four characteristic PAHs congeners. Dashed lines in the plots are linear regressions.

also be dependent on their environmental behaviors including sorption and biodegradation in addition to their emissions. In previous study[46], significant linear relationships between the concentrations of sixteen PAHs in sediments (C_{PAHs}) with their emissions (E_{PAHs}) were established (Eq. 10). Moreover, positive and negative relationships of **K** (Eq. 11) and **L** (Eq. 12) with $\log K_{ow}$ were established, respectively.

$$C_{PAHs} = K \times E_{PAHs} + L \tag{10}$$

$$K = 3E - 06 \times \log K_{ow}^{8.24}$$
$$\left(N = 16,\ F = 427,\ R^2 = 0.93, p < 0.01 \right) \tag{11}$$

$$L = -117.41(\pm 12.48) \times \log K_{ow} + 416.16(\pm 58.13)$$
$$\left(N = 16,\ F = 384,\ R^2 = 0.86, p < 0.01 \right) \tag{12}$$

In this study, a multilinear relationship of $C_{\Sigma PAHs}$ with C_{Nap}, C_{Acy}, C_{Phe}, and C_{BaA} was established (Eq. 8). The concentration of four characteristic PAHs congeners in sediments can be calculated using their emissions and $\log K_{ow}$ (Eqs. 10–12). Therefore, $C_{\Sigma PAHs}$ in sediments can be predicted using the emissions and $\log K_{ow}$ of four characteristic PAHs congeners, in which $\log K_{ow}$ can be accounted for PAHs partition ability. Mean $C_{\Sigma PAHs(exp)}$ in surface sediments sampled in investigated provinces of China (N = 30) and other countries (N = 21) versus $C_{\Sigma PAHs(cal)}$ predicted using E_{PAHs} (Tables S7 and S8) and $\log K_{ow}$ of four characteristic PAHs congeners is presented in Fig. 8. The SDEV value between $C_{\Sigma PAHs(exp)}$ and $C_{\Sigma PAHs(cal)}$ is 54%, suggesting that $C_{\Sigma PAHs(cal)}$ are well consistent with $C_{\Sigma PAHs(exp)}$. Therefore, the established model in this study can be used to predict $C_{\Sigma PAHs}$ in sediments with high accuracy, resulting in decreasing cost of laboratory analysis.

The correlations that have been previously described in literature of $C_{\Sigma PAHs}$ with C_{BaP}[36,37], C_{Pyr}[38] or C_{Ace}[39] could be attributed to the PAHs emissions in the investigated region from one emission source or emission sources with similar EFs (Table 1). For example, PAHs in sediment samples of Norway were mainly from manufactured gas plants and aluminum smelters[38], in which Pyr is the dominant congener with relatively high EFs[40,41,52]. However, the multiple linear relationship established herein (Eq. 6) gives a useful way to predict the $C_{\Sigma PAHs}$ in sediments using PAHs emissions emitted from major emission sources around the world as seen by the good correlation with the large and diverse sample size. Therefore, this relationship would be valuable for predicting total PAHs concentrations and assessing their risks in sediments.

Conclusion and perspectives

A multiple linear relationship of $C_{\Sigma PAHs}$ with C_{Nap}, C_{Acy}, C_{Phe}, and C_{BaA} in sediments was established employing the reported data in the past 30 years. This suggested the selected four PAHs congeners, including Nap, Acy, Phe, and BaA, are the characteristic congeners in sediments. Moreover, the multiple linear relationship of $EF_{\Sigma PAHs}$ with the EFs of the four congeners was also developed. The same characteristic congeners observed for PAHs in sediments and in emission sources indicates that the concentration of PAHs in sediments are largely dependent on their emissions. Additionally, the ratio of multicomponents coefficient from the multiple linear relationship in sediments to that from the multiple linear relationship in emission sources correlated positively with $\log K_{ow}$ of the four congeners. Therefore, a model for predicting $C_{\Sigma PAHs}$ in sediments was established using the emissions
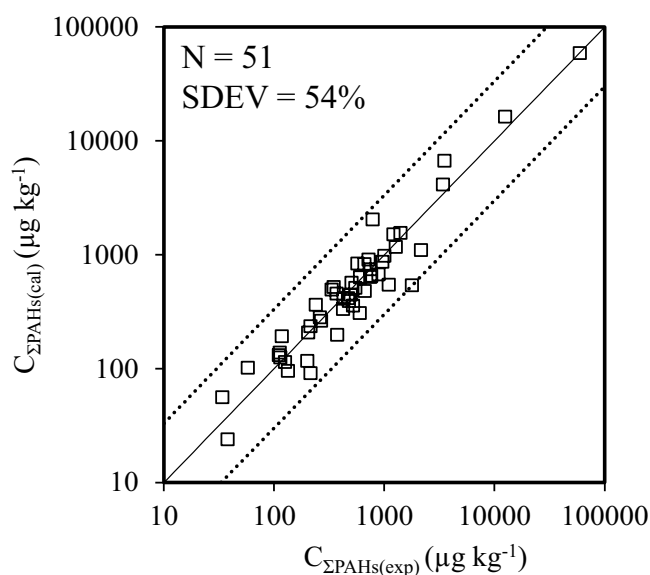
Figure 8. Fitted $C_{\Sigma PAHs(cal)}$ using E_{PAHs} and $\log K_{ow}$ of four characteristic PAHs congeners versus $C_{\Sigma PAHs(exp)}$ in sediments sampled in investigated provinces of China and other countries. The y = x line (solid line) indicates a 1:1 relationship between $C_{\Sigma PAHs(cal)}$ and $C_{\Sigma PAHs(exp)}$. Dashed lines in plots indicate the SDEV values from the reference lines.

and $\log K_{ow}$ of four PAHs congeners. The SDEV value between $C_{\Sigma PAHs(exp)}$ and $C_{\Sigma PAHs(cal)}$ was 54%, suggesting the established model can accurately predict $C_{\Sigma PAHs}$ in sediments.

Although the relationship established in this study could be used to predict total sixteen PAHs concentration in surface sediments of China and other countries, the application of this method for predicting additional PAHs in sediment, such as alkylated-PAHs, needs further verified.

Methodology

Literature search. Concentration data of sixteen parent PAHs (Table S4 and Table S6) in global bottom sediments of fresh water reported in the past 30 years were collected. A systematic literature retrieval was performed using the ISI Web of Science database, Google®Scholar, WanFang Data of E-Resources and China Knowledge Resource Integrated Database including master/doctoral dissertation using the terms of "polycyclic aromatic hydrocarbons" or "PAHs" and "sediment/sediments" as the primary keywords[60]. Articles were then examined individually to ensure that the duplicates and irrelevant articles were excluded from further analysis. In addition, articles without individual PAHs concentration data and/or articles that did not report QA/QC procedure and limits of detection (LODs) were also excluded from further analysis[60]. In order to perform the required comparisons in this study, it was assumed that there were no significant differences in the sampling process and analysis among the investigating groups/laboratories[60,61]. In total, 22,349 individual PAH concentrations from 1445 sediments samples were collected from 1184 publications and then used for meta-analysis (Table S4 and Table S6).

PAHs emissions. According to the previous study[40], PAHs emissions in globe was primarily emitted from coking production, petroleum refineries, domestic and industrial coal combustion, straw and firewood burning, iron-steel industry, transport petroleum, and primary Al production, which accounting for more than 92% of all source contributions. Therefore, PAHs emissions from these nine sources were calculated using a previously reported approach for analysis[40,41]. Emission factors (EFs, g t^{-1}) of sixteen PAHs from above nine emission sources were summarized in Table S5. Provincial and national PAHs emissions (E_{PAHs}, t a^{-1}) were calculated using Eq. (13)[40,41,52]:

$$EPAHs = \sum_{k,l} EFi,j,k \times Xj,k \times Ak \tag{13}$$

where i, j, and k represent each PAH congener, sources, and technology, respectively.

EF (g t^{-1}) is the emission factor of the PAHs congener i (Table S5). X is the fraction of the activity rate contributed by a given technology j, which was calculated using the technology split method[40,41,52]. Activity data (A, 10^4 t a^{-1}) in source j, from China, were obtained directly from China Statistical Yearbook (2001–2018) and China Energy Statistical Yearbook (2001–2018), edited by National Bureau of Statistics[40]. The data from other countries were derived from Food and Agriculture Organization of the United Nations, International Yearbook of Industrial Statistics (2004–2018), and International Energy Agency World Energy Statistics and Balances[40].

For the technology splitting approach, six sources (coking production, industrial coal combustion, indoor straw and firewood burning, iron-steel industry, and primary Al production) were divided into two or three

divisions with or without different emission mitigation measures[40,41]. For the remaining three sources, fixed EF_{PAHs} without divisions were used[40,41]. The time-dependent fractions of technology divisions were calculated using a series of S-shaped curves (Eq. 14, Table S9).

$$X(t) = \left(X_0 - X_f\right)e^{-\frac{(t-t_0)^2}{2s^2}} + X_f \tag{14}$$

where X_0 and X_f are initial and final fractions of a certain technology division, respectively. t_0 is the start time of technology transition, and s is a rate. The X_f, X_0, t_0, and s were illustrated in Table S9[40].

Data analysis. 11,937 individual concentrations data from 754 sediments sampled from China were used to establish the relationship between $C_{\Sigma PAHs}$ and the concentration of selected congeners in sediments (Table S4). To validate the established relationship, 10,412 individual concentrations data from 691 sediments sampled from globe (excluding China) were used as a test set (Table S6). Concentrations that were reported to be below the method LODs were assigned half the value of the reported LODs[61,62]. Concentration unit of PAHs were set uniformly to micrograms per kilogram ($\mu g\ kg^{-1}$) of dry weight. Prior to statistical analysis, a histogram with normal curve was viewed and a Kolmogorov–Smirnov test were performed to verify the normality of variables[38]. If the significance (p) is greater than 0.05 ($p > 0.05$), it can be judged that the variables are normal[38]. Hierarchical clustering analysis (HCA) and classifications were performed using the SPSS Statistics 19.0 software (Version 19.0, Chicago, IL, USA) according to relative similarities of EFs in emission sources and concentrations in sediments of sixteen PAHs[42,43]. Statistical analysis, including linear and multilinear regression, were also performed using the SPSS Statistics 19.0 with a critical significance (p) up to 0.05 to check significance. Provincial or national PAHs emissions combined with their observed $C_{\Sigma PAHs}$ in surface sediments were used to evaluate the established model between $C_{\Sigma PAHs}$ and emissions of the four characteristic congeners. Moreover, $C_{\Sigma PAHs}$ in surface sediments sampled in the same province or nation at the same year were expressed by the geometric mean value[63].

Percent sample deviation (SDEV, Eq. (15)) was calculated based on the relative error between the experimental values (C_{exp}) and the calculated value (C_{cal})[64]. In addition to the SDEV, significance of F test (p) and correlation coefficient (R^2) were used to evaluate the goodness of the fitting and the established correlations by regression analysis[64].

$$SDEV = \sqrt{\frac{\sum \left(\frac{C_{cal} - C_{exp}}{C_{exp}}\right)^2}{N - k} \times 100} \tag{15}$$

where N is the number of experimental values and k is the number of predictors for linear regression.

References

1. Haritash, A. K. & Kaushik, C. P. Biodegradation aspects of polycyclic aromatic hydrocarbons (PAHs): A review. *J. Hazard. Mater.* **169**, 1–15 (2009).
2. Zheng, X. *et al.* Characterizing particulate polycyclic aromatic hydrocarbon emissions from diesel vehicles using a portable emissions measurement system. *Sci. Rep.* **7**, 10058 (2017).
3. Syed, J. H. *et al.* Polycyclic aromatic hydrocarbons (PAHs) in Chinese forest soils: Profile composition, spatial variations and source apportionment. *Sci. Rep.* **7**, 2692 (2017).
4. Agarwal, T., Khillare, P. S. & Shridhar, V. Pattern, sources and toxic potential of PAHs in the agricultural soils of Delhi, India. *J. Hazard. Mater.* **163**, 1033–1039 (2009).
5. Chen, W. H., Hsieh, M. T., You, J. Y., Quadir, A. & Lee, C. L. Temporal and vertical variations of polycyclic aromatic hydrocarbon at low elevations in an industrial city of southern Taiwan. *Sci. Rep.* **11**, 3453 (2021).
6. Vu, V. T., Lee, B. K., Kim, J. T., Lee, C. H. & Kim, I. H. Assessment of carcinogenic risk due to inhalation of polycyclic aromatic hydrocarbons in PM_{10} from an industrial city: A Korean case-study. *J. Hazard. Mater.* **189**, 349–356 (2011).
7. Li, S. Y., Tao, Y. Q., Yao, S. C. & Xue, B. Distribution, sources, and risks of polycyclic aromatic hydrocarbons in the surface sediments from 28 lakes in the middle and lower reaches of the Yangtze River region, China. *Environ. Sci. Pollut. Res.* **23**, 4812–4825 (2016).
8. Bergamasco, A. *et al.* Composition, distribution, and sources of polycyclic aromatic hydrocarbons in sediments of the Gulf of Milazzo (Mediterranean Sea, Italy). *Polycycl. Aromat. Hydrocarb.* **34**, 397–424 (2014).
9. Portet-Koltalo, F. *et al.* Bioaccessibility of polycyclic aromatic compounds (PAHs, PCBs) and trace elements: Influencing factors and determination in a river sediment core. *J. Hazard. Mater.* **384**, 121499 (2020).
10. Doong, R. A. & Lin, Y. T. Characterization and distribution of polycyclic aromatic hydrocarbon contaminations in surface sediment and water from Gao-ping River, Taiwan. *Water Res.* **38**, 1733–1744 (2004).
11. Chen, Y. Y., Zhu, L. Z. & Zhou, R. B. Characterization and distribution of polycyclic aromatic hydrocarbon in surface water and sediment from Qiantang River, China. *J. Hazard. Mater.* **141**, 148–155 (2007).
12. Guo, W. *et al.* Distribution, partitioning and sources of polycyclic aromatic hydrocarbons in Daliao River water system in dry season, China. *J. Hazard. Mater.* **164**, 1379–1385 (2009).
13. Maskaoui, K., Zhou, J. L., Hong, H. S. & Zhang, Z. L. Contamination by polycyclic aromatic hydrocarbons in the Jiulong River Estuary and Western Xiamen Sea, China. *Environ. Pollut.* **118**, 109–122 (2002).
14. Tian, Y. Z., Li, W. H., Shi, G. L., Feng, Y. C. & Wang, Y. Q. Relationships between PAHs and PCBs, and quantitative source apportionment of PAHs toxicity in sediments from Fenhe reservoir and watershed. *J. Hazard. Mater.* **248–249**, 89–96 (2013).
15. Adhikari, P., Maiti, K., Overton, E., Rosenheim, B. & Marx, B. Distributions and accumulation rates of polycyclic aromatic hydrocarbons in the northern Gulf of Mexico sediments. *Environ. Pollut.* **212**, 413–423 (2016).

16. Cardoso, F. D., Dauner, A. L. L. & Martins, C. C. Critical and comparative appraisal of polycyclic aromatic hydrocarbons in sediments and suspended particulate material from a large South American subtropical estuary. *Environ. Pollut.* **214**, 219–229 (2016).
17. Montuori, P. *et al.* Distribution, sources and ecological risk assessment of polycyclic aromatic hydrocarbons in water and sediments from Tiber River and estuary, Italy. *Sci. Total Environ.* **566–567**, 1254–1267 (2016).
18. Xu, E. G., Bui, C., Lamerdin, C. & Schlenk, D. Spatial and temporal assessment of environmental contaminants in water, sediments and fish of the Salton Sea and its two primary tributaries, California, USA, from 2002 to 2012. *Sci. Total Environ.* **559**, 130–140 (2016).
19. Martinez, E., Gros, M., Lacorte, S. & Barceló, D. Simplified procedures for the analysis of polycyclic aromatic hydrocarbons in water, sediments and mussels. *J. Chromatogr. A* **1047**, 181–188 (2004).
20. Leite, N. F., Peralta-Zamora, P. & Grassi, M. T. Multifactorial optimization approach for the determination of polycyclic aromatic hydrocarbons in river sediments by gas chromatography–quadrupole ion trap selected ion storage mass spectrometry. *J. Chromatogr. A* **1192**, 273–281 (2008).
21. Pena-Abaurrea, M., Ye, F., Blasco, J. & Ramos, L. Evaluation of comprehensive two-dimensional gas chromatography-time-of-flight-mass spectrometry for the analysis of polycyclic aromatic hydrocarbons in sediments. *J. Chromatogr. A* **1256**, 222–231 (2012).
22. Song, Y. F., Jing, X., Fleischmann, S. & Wilke, B. M. Comparative study of extraction methods for the determination of PAHs from contaminated soils and sediments. *Chemosphere* **48**, 993–1001 (2002).
23. Shamsipur, M. & Hassan, J. A novel miniaturized homogenous liquid–liquid solvent extraction-high performance liquid chromatographic-fluorescence method for determination of ultra traces of polycyclic aromatic hydrocarbons in sediment samples. *J. Chromatogr. A* **1217**, 4877–4882 (2010).
24. Frenna, S., Mazzola, A., Orecchio, S. & Tuzzolino, N. Comparison of different methods for extraction of polycyclic aromatic hydrocarbons (PAHs) from Sicilian (Italy) coastal area sediments. *Environ. Monit. Assess.* **185**, 5551–5562 (2013).
25. Liu, Y., Kong, X., Zhang, Y. & Zhang, Y. Analysis on the purification technology of dichloromethane waste gas. *Appl. Chem. Ind.* **50**, 1409–1413 (2021).
26. Cooper, G. S., Scott, C. S. & Bale, A. S. Insights from epidemiology into dichloromethane and cancer risk. *Int. J. Environ. Res. Public Health* **8**, 3380–3398 (2011).
27. Owen, C. *et al.* Screening for PAHs by fluorescence spectroscopy: A comparison of calibrations. *Chemosphere* **31**, 3345–3356 (1995).
28. Peterson, G. S., Axler, R. P., Lodge, K. B., Schuldt, J. & Crane, J. Evaluation of a fluorometric screening method for predicting total PAH concentrations in contaminated sediments. *Environ. Monit. Assess.* **78**, 111–129 (2002).
29. Simpson, C. D., Mosi, A. A., Cullen, W. R. & Reimer, K. J. Composition and distribution of polycyclic aromatic hydrocarbon contamination in surficial marine sediments from Kitimat Harbor, Canada. *Sci. Total Environ.* **181**, 265–278 (1996).
30. Sun, J. *et al.* Distribution of polycyclic aromatic hydrocarbons (PAHs) in Henan Reach of the Yellow River, Middle China. *Ecotoxicol. Environ. Saf.* **72**, 1614–1624 (2009).
31. Arienzo, M. *et al.* Characterization and source apportionment of polycyclic aromatic hydrocarbons (PAHs) in the sediments of gulf of Pozzuoli (Campania, Italy). *Mar. Pollut. Bull.* **124**, 480–487 (2017).
32. Chiou, C. T., McGroddy, S. E. & Kile, D. E. Partition characteristics of polycyclic aromatic hydrocarbons on soils and sediments. *Environ. Sci. Technol.* **32**, 264–269 (1998).
33. Bucheli, T. D., Blum, F. & Desaules, A. Polycyclic aromatic hydrocarbons, black carbon, and molecular markers in soils of Switzerland. *Chemosphere* **56**, 1061–1076 (2004).
34. Cornelissen, G., Gustafsson, O. & Bucheli, T. D. Extensive sorption of organic compounds to black carbon, coal, and kerogen in sediments and soils: Mechanisms and consequences for distribution, bioaccumulation, and biodegradation. *Environ. Sci. Technol.* **39**, 6881–6895 (2005).
35. Jin, J. *et al.* Characterization and phenanthrene sorption of natural and pyrogenic organic matter fractions. *Environ. Sci. Technol.* **51**, 2635–2642 (2017).
36. Zhu, L. Z., Chen, B. L., Shen, H. X. & Wang, J. Pollution status quo and risk of polycyclic aromatic hydrocarbons in surface water of Hangzhon City, China. *Environ. Sci.* **23**, 485–489 (2003) (**(in Chinese)**).
37. Luo, S. Study on the organic pollution status and source apportionment of PAHs in water and sediment of HongFeng Lake. Master. Guizhou Normal University, pp. 87 (2005).
38. Arp, H., Azzolina, N., Cornelissen, G. & Hawthorne, S. Predicting pore water EPA-34 PAH concentrations and toxicity in pyrogenic-impacted sediments using pyrene content. *Environ. Sci. Technol.* **45**, 5139–5146 (2011).
39. Qian, X., Liang, B., Fu, W., Liu, X. & Cui, B. Polycyclic aromatic hydrocarbons (PAHs) in surface sediments from the intertidal zone of Bohai Bay, Northeast China: Spatial distribution, composition, sources and ecological risk assessment. *Mar. Pollut. Bull.* **112**, 349–358 (2016).
40. Shen, H. *et al.* Global atmospheric emissions of polycyclic aromatic hydrocarbons from 1960 to 2008 and future predictions. *Environ. Sci. Technol.* **47**, 6415–6424 (2013).
41. Li, B. *et al.* An improved gridded polycyclic aromatic hydrocarbon emission inventory for the lower reaches of the Yangtze River Delta region from 2001 to 2015 using satellite data. *J. Hazard. Mater.* **360**, 329–339 (2018).
42. Sørlie, T., Perou, C. M. & Tibshirani, R. Gene expression patterns of breast carcinomas distinguish tumor subclasses with clinical implications. *PNAS* **98**, 10869–10874 (2001).
43. Oh, J. E., Gullett, B., Ryan, S. & Touati, A. Mechanistic relationships among PCDDs/Fs, PCNs, PAHs, CIPhs, and CIBzs in municipal waste incineration. *Environ. Sci. Technol.* **41**, 4705–4710 (2007).
44. Liu, G. *et al.* Identification of indicator congeners and evaluation of emission pattern of polychlorinated naphthalenes in industrial stack gas emissions by statistical analyses. *Chemosphere* **118**, 194–200 (2015).
45. Zhang, W. T. & Dong, W. Chapter 6 - Advanced course of SPSS statistical analysis, Beijing, Higher Education Press, pp 97–108 (2013).
46. Wang, W. W., Qu, X. L., Lin, D. H. & Yang, K. Octanol-water partition coefficient (logK$_{ow}$) dependent movement and time lagging of polycyclic aromatic hydrocarbons (PAHs) from emission sources to lake sediments: A case study of Taihu Lake, China. *Environ. Pollut.* **288**, 117709 (2021).
47. Li, R., Hua, P., Zhang, J. & Krebs, P. A decline in the concentration of PAHs in Elbe River suspended sediments in response to a source change. *Sci. Total Environ.* **663**, 438–446 (2019).
48. Moeckel, C., Monteith, D. T., Llewellyn, N. R., Henrys, P. A. & Pereira, M. G. Relationship between the concentrations of dissolved organic matter and polycyclic aromatic hydrocarbons in a typical U.K. upland stream. *Environ. Sci. Technol.* **48**, 130–138 (2014).
49. Feng, J., Zhai, M. & Sun, J. Distribution and sources of polycyclic aromatic hydrocarbons (PAHs) in sediment from the upper reach of Huaihe River, East China. *Environ. Sci. Pollut. Res.* **19**, 1097–1106 (2012).
50. Zhang, J., Liu, G., Wang, R. & Liu, J. Distribution and source apportionment of polycyclic aromatic hydrocarbons in bank soils and river sediments from the middle reaches of the Huaihe River, China. *CSAWAC* **43**, 1115–1266 (2015).
51. Zheng, X. Contamination and release kinetics of polycyclic aromatic hydrocarbons (PAHs) in Beijing-Hangzhou Grand Canal (Subei Section). China Mining University (2010).
52. Li, B. *et al.* New method for improving spatial allocation accuracy of industrial energy consumption and implications for polycyclic aromatic hydrocarbon emissions in China. *Environ. Sci. Technol.* **53**, 4326–4334 (2019).
53. Xu, S. S., Liu, W. X. & Tao, S. Emission of polycyclic aromatic hydrocarbons in China. *Environ. Sci. Technol.* **40**, 702–708 (2006).

54. Witt, G. & Trost, E. Polycyclic aromatic hydrocarbons (PAHs) in sediments of the Baltic Sea and of the German coastal waters. *Chemosphere* **38**, 1603–1614 (1999).
55. Viguri, J., Verde, J. & Irabien, A. Environmental assessment of polycyclic aromatic hydrocarbons (PAHs) in surface sediments of the Santander Bay, Northern Spain. *Chemosphere* **48**, 157–165 (2002).
56. Replinger, S., Katka, S., Toll, J., Church, B. & Saban, L. Recommendations for the derivation and use of biota-sediment bioaccumulation models for carcinogenic polycyclic aromatic hydrocarbons. *Integr. Environ. Asses.* **13**, 1060–1071 (2017).
57. Maletić, S. P., Beljin, J. M., Rončević, S. D., Grgić, M. G. & Dalmacija, B. D. State of the art and future challenges for polycyclic aromatic hydrocarbons is sediments: sources, fate, bioavailability and remediation techniques. *J. Hazard. Mater.* **365**, 467–482 (2019).
58. Bacosa, H. P. & Inoue, C. Polycyclic aromatic hydrocarbons (PAHs) biodegradation potential and diversity of microbial consortia enriched from tsunami sediments in Miyagi, Japan. *J. Hazard. Mater.* **283**, 689–697 (2015).
59. Johnsen, A. R., Wick, L. Y. & Harms, H. Principles of microbial PAH-degradation in soil. *Environ. Pollut.* **133**, 71–84 (2005).
60. Bu, Q., Wang, B., Huang, J., Deng, S. & Yu, G. Pharmaceuticals and personal care products in the aquatic environment in China: A review. *J. Hazard. Mater.* **262**, 189–211 (2013).
61. Ma, W. L. *et al.* Polycyclic aromatic hydrocarbons in Chinese surface soil: occurrence and distribution. *Environ. Sci. Pollut. Res.* **22**, 4190–4200 (2015).
62. Cai, Q. Y., Mo, C. H., Wu, Q. T., Katsoyiannis, A. & Zeng, Q. Y. The status of soil contamination by semivolatile organic chemicals (SVOCs) in China: A review. *Sci. Total Environ.* **389**, 209–224 (2008).
63. Yu, H. *et al.* Polycyclic aromatic hydrocarbons in surface freshwaters from the seven main river basins of China: Spatial distribution, source apportionment, and potential risk assessment. *Sci. Total Environ.* **752**, 141764 (2021).
64. Crittenden, J. C. *et al.* Correlation of aqueous-phase adsorption isotherms. *Environ. Sci. Technol.* **33**, 2926–2933 (1999).

Acknowledgements

Author contributions

W.W.: writing-original draft. H.X.: writing-review and editing. X.Q.: writing-review and editing. D.L.: writing-review and editing. K.Y.: supervision, writing-review and editing.

Competing interests

The authors declare no competing interests.

Additional information

Supplementary Information The online version contains supplementary material available at https://doi.org/10.1038/s41598-022-07312-2.

Correspondence and requests for materials should be addressed to K.Y.

Reprints and permissions information is available at www.nature.com/reprints.

Publisher's note Springer Nature remains neutral with regard to jurisdictional claims in published maps and institutional affiliations.